Journal of Micromechanics and Microengineering

The shape of a step structure as a design aspect to control droplet generation in microfluidics

To cite this article: S P C Sim *et al* 2010 *J. Micromech. Microeng.* **20** 035010

J. Micromech. Microeng. **20** (2010) 035010 (6pp) doi:10.1088/0960-1317/20/3/035010

The shape of a step structure as a design aspect to control droplet generation in microfluidics

S P C Sim[1], T G Kang[1], L Yobas[1,4], C Holtze[2] and D A Weitz[3]

[1] Institute of Microelectronics, A*STAR (Agency for Science, Technology and Research), Singapore
[2] BASF, 67056 Ludwigshafen, Germany
[3] Department of Physics, Harvard University, Cambridge, MA 02138, USA

E-mail: leventy@ime.a-star.edu.sg

Received 19 August 2009, in final form 25 November 2009
Published 9 February 2010
Online at stacks.iop.org/JMM/20/035010

Abstract
In this paper, silicon-based devices with a step structure integrated at the flow-focusing junction were designed, fabricated and characterized for droplet generation. A two-step silicon etching method was demonstrated to create the step structure. During fabrication, undesirable spikes encountered at the step edge were removed by oxygen plasma ashing and silicon isotropic etching. With this method, two types of step profile (flat and triangular profiles) were fabricated. These two profiles were compared for their differences in droplet-generation behavior. The device with the flat-step profile was found to make larger droplets and at a lower frequency compared to the device with the triangular-step profile. Additionally, polydimethylsiloxane and glass were tested as capping materials for the devices and the impact of their surface characteristics (hydrophobic and hydrophilic) on the type of droplets (water-in-oil or oil-in-water) formed was investigated.

(Some figures in this article are in colour only in the electronic version)

1. Introduction

Emulsions or droplets play a defining role for acceptability and quality of products in various industries such as food [1], cosmetics [2] and pharmaceuticals [3]. A uniform size distribution of emulsions increases their stability. Unlike conventional methods, microfluidic devices are capable of producing exceptionally monodisperse droplets [4]. Given such uniformity, these devices have now been considered for manufacturing stable emulsions.

In principle, droplet formation in microfluidic devices makes use of either cross-flow [5–7] or flow-focusing junctions [8, 9]. The former generates droplets by crossing the streams of two immiscible liquids whereas the latter generates droplets by co-flowing the streams through a narrow opening. Varying the flow rates of the streams allows control over the average size of the droplets generated. At a low flow rate, droplets are formed in dripping mode directly at the junction [8]. At a high flow rate, the dispersed phase extends a stable thread further downstream of the junction where the thread breaks into droplets due to the Rayleigh–Plateau instability [8]. This is known as jetting [10].

Geometrical variations introduced in these designs further enhance droplet monodispersity and/or throughput. For example, a planar nozzle profile has been introduced to create a point of maximized shear-stress gradient along a flow-focusing junction where discrete droplets break free consistently [11]. This structure has been extended to a three-dimensional profile with the integration of a circular sharp orifice in a flow-focusing configuration [12, 13]. In another configuration, a step positioned at the junction downstream breaks a liquid thread emanating from a junction into droplets due to sudden expansion [10, 14, 15].

Besides improving monodispersity and throughput, new geometries of microchannels are also studied to overcome the limitation of surface wettability. Empirically, water-in-oil (W/O) droplets are formed in hydrophobic channels while oil-in-water (O/W) droplets are formed in hydrophilic channels [9]. To relax this limitation, coaxial flow-focusing geometries

[4] Author to whom any correspondence should be addressed.

[16–18] have been employed so that W/O or O/W droplets can be made independent of the surface wettability. This implementation will avoid the difficult modifications of surface wettability [19, 20] altogether; this is of particular value since it is often very difficult to make the surface treatments sufficiently robust to maintain the wetting characteristics over the lifetime of the device. Another benefit of these geometries is that double emulsions (O/W/O and W/O/W droplets) could be easily made in microchannels with a single wettability character. No dual wettability character (hydrophilic downstream and hydrophobic upstream or the opposite) in the microchannels is required to make the desired type of double emulsions.

Here, we integrate step geometries directly at a flow-focusing junction in silicon-based platforms to investigate the effect of geometry in the production of droplets and its implication on wettability. In this design, silicon-based devices capped with either glass or polydimethylsiloxane (PDMS) were fabricated and studied. To fabricate the step-profile at the flow-focusing junction, a two-step silicon etching method was used. This method was also utilized to make two different profiles (flat and triangular) for the step structure. With the fabricated devices, droplets were generated and the droplet generation behavior was characterized.

2. Methods

In each of our devices, the step structure was positioned directly at the flow-focusing junction as described in figure 1. The microchannel prior to the junction was 200 μm wide (w) and 50 μm deep (h_1) whereas the step was 50 μm high (h_2). Two distinct step profiles were implemented: a single flat edge and a triangular edge (two slanted edges converging at an angle of 90°).

To integrate a step profile into the flow-focusing junction, a two-step dry etch process was used with the first etch step initiating the channels at the downstream of the junction whereas the second etch step creating the upstream channels as well as the step structure. The process utilized 200 mm silicon wafers with a dual layer of SiO_2 each deposited and patterned 5000 Å thick (figures 2(*a*) and (*b*)). The first silicon etch was carried out by deep reactive-ion etching (DRIE) to create 50 μm deep trenches (figure 2(*c*)). After DRIE, the top SiO_2 was stripped away by a time-controlled etch. Upon exposure of the silicon substrate, the second silicon etch step was also performed with DRIE to create an additional 50 μm depth (figure 2(*d*)). This created the step structure and the trenches upstream of the junction. Oxygen plasma cleaning followed by silicon isotropic etching was then used to remove undesired spikes formed at the edge of the step structure. The remaining SiO_2 layer was then removed. Subsequently, a 3000 Å thick SiO_2 layer (figure 2(*e*)) was deposited on the silicon surface to make the surface hydrophilic. Fluidic feed-through holes were laser drilled. The devices were completed by capping the microchannels with plain glass using anodic bonding.

The devices as fabricated had hydrophilic microchannel walls. For hydrophobic walls, the devices were treated with silane (1H, 1H, 2H, 2H perfluorooctyltriethoxysilane 98%, Aldrich) using the chemical vapor deposition (CVD) method. The contact angle of water after silanization was 107.8° (Kruss contact angle instrument, DSA100).

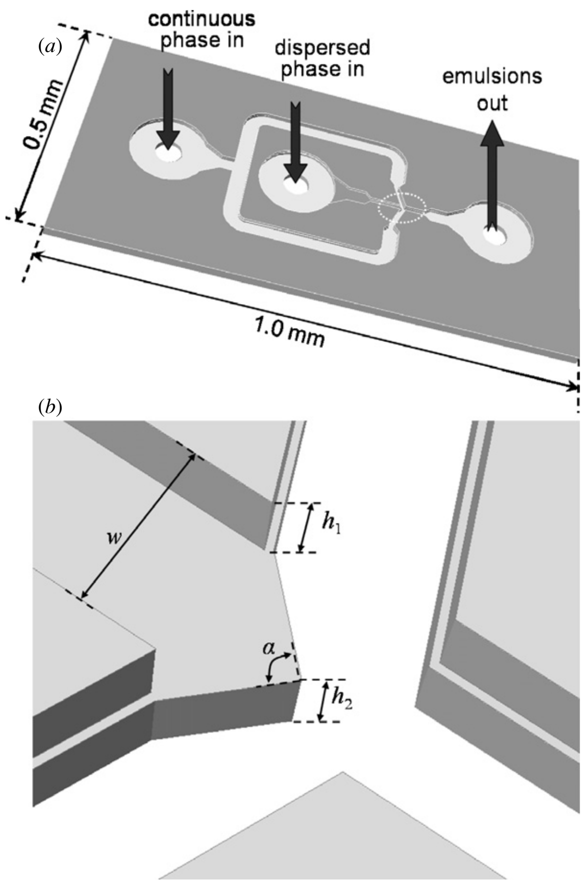

Figure 1. Schematics of (*a*) the overall device and (*b*) the scaled-up flow-focusing junction having a triangular step ($h_1 = h_2 = 50$ μm, $w = 200$ μm, and $\alpha = 90°$).

Alternatively, some of our devices were capped with a PDMS layer. In this case, the silicon substrate was prepared as before (figures 2(*a*)–(*e*)), skipping the laser drilling step. Upon depositing a layer of SiO_2 on the silicon substrate (figure 2(*e*)), a planar PDMS cover (with holes punched through for fluidic interconnects) was then aligned and bonded to the silicon substrate through oxygen–plasma surface activation. For the hydrophilic PDMS surface, the devices were used directly after oxygen plasma bonding [21]. For hydrophobic PDMS surface, the devices were left overnight in ambient environment to let them regain their hydrophobic nature.

In our experimental setup, a customized acrylic housing was used to hold the devices capped with glass. The housing provided the respective fluidic interconnections for the continuous and dispersed phase flows, and for the collection of droplets (figure 3). For device characterization, either O/W or W/O droplets were generated. The oil was pure silicone oil (Dow Corning 200 fluid, 20 cSt) and the aqueous phase was a commercial aqueous food dye solution (used neat without dilution or the addition of surfactant). These fluids were dispensed using syringe pumps. A computer-aided high-speed camera (Photron, APX-RS) coupled with a microscope was used to capture images and videos of the droplet generation

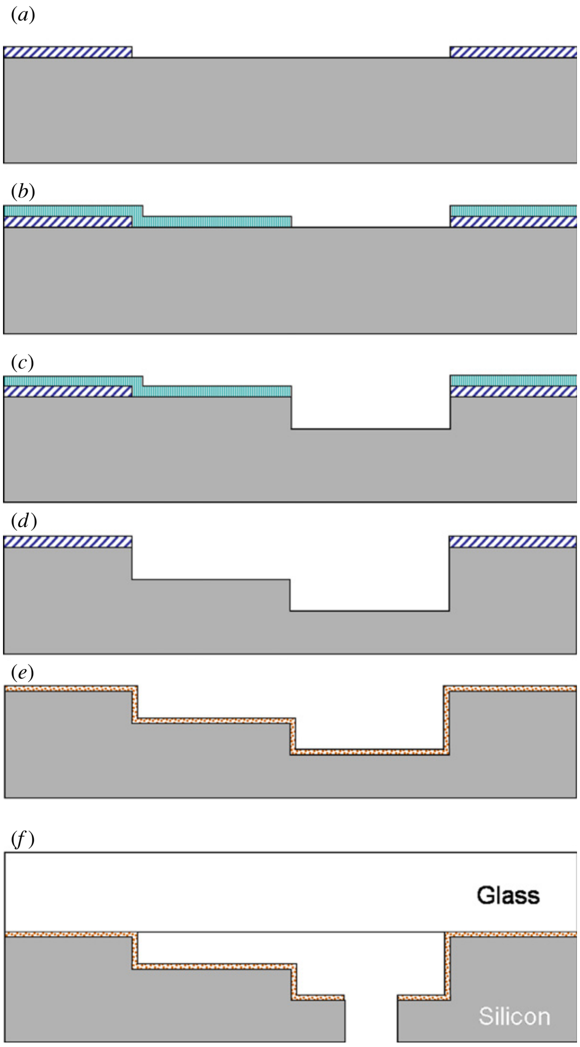

Figure 2. Cross-sectional schematics of the device shown after the microfabrication steps: (*a*) patterning of the first 5000 Å thick SiO_2 layer; (*b*) patterning of the second 5000 Å thick SiO_2 layer; (*c*) 50 μm deep DRIE; (*d*) stripping of the top SiO_2 layer and 50 μm deep DRIE, (*e*) stripping of the remaining SiO_2 and deposition of 3000 Å thick SiO_2 layer; (*f*) laser drilling holes and glass anodic bonding.

process. Using the captured images, the average diameter of the droplets was estimated using an imaging software (ImageJ). With the measured diameter, the volume of the droplets was calculated assuming that each droplet had a discoid shape when the diameter was larger than the channel height [22]. The frequency of droplet generation was derived by counting the number of droplets generated for a specific duration in the captured video clips.

The same setup was also utilized for the devices capped with PDMS. In this case, no acrylic housing was needed. Instead, tubes from the syringes were directly plugged into the holes through the PDMS.

3. Results and discussions

The flow-focusing junction with a step structure was fabricated using a two-step silicon etching process. In this method, undesired silicon spikes appeared at the edge of the step structure (figure 4(*a*) inset). The spikes were caused by the passivation residue from the fist DRIE process where the passivation and directional etching steps alternated in cycles. In the last cycle, the etchant attacked the passivation layer at the trench bottom, leaving the passivation at the trench sidewalls intact. The intact passivation consequently acted as a masking layer for the second DRIE step. This led to the formation of spikes. In order to remove the spikes, a combination of oxygen plasma ashing and silicon isotropic etching was applied.

Through the fabrication process described, mainly two different step profiles (flat and triangular) were produced (figure 4).

Using the devices capped with glass, the two distinct step profiles including the device without a step profile were

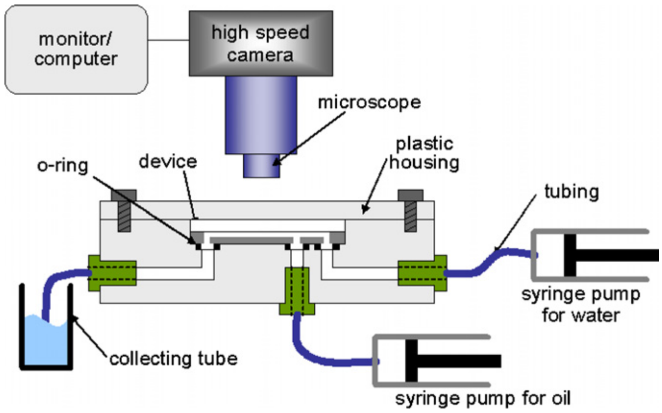

Figure 3. Schematic of the experimental test setup showing injection of immiscible liquids into the device from syringe pumps and monitoring of the flow-focusing junction through high-speed video microscopy.

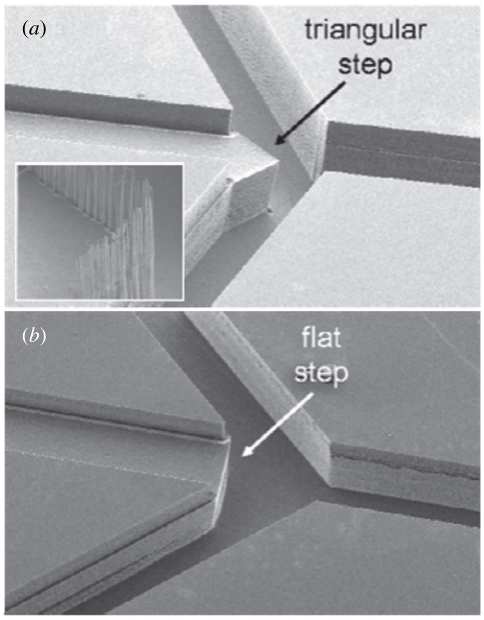

Figure 4. SEM images of the flow-focusing junctions incorporating a (*a*) triangular and (*b*) flat step profile. The inset shows the silicon spikes formed during etching the step profile but then cleared by isotropic etching.

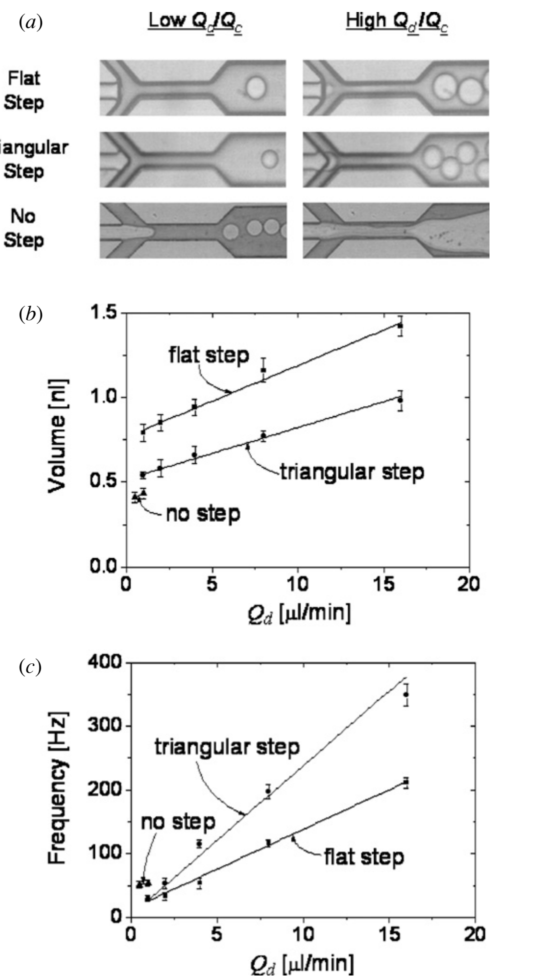

Figure 5. (*a*) Formation of O/W droplets in devices with and without a step structure at a ratio of Q_d/Q_c low (0.025) and high (0.4). Thread flow formation instead of droplets was observed at high Q_d/Q_c for the device without a step. Plots of (*b*) volume and (*c*) generation frequency of the droplets as a function of Q_d at a fixed Q_c (40 μL min^{-1} for the devices with a step or 20 μL min^{-1} without a step). The device without a step exhibits a narrow working range (limited to low Q_d) in which droplets can be generated. Beyond this range, no droplet can be formed.

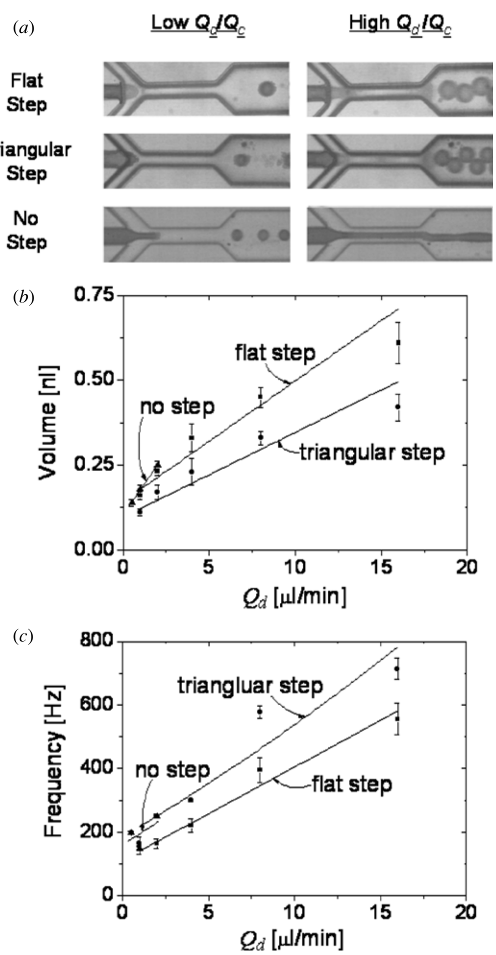

Figure 6. (*a*) Formation of W/O droplets in devices with and without a step structure at a ratio of Q_d/Q_c low (0.025) and high (0.4). Thread flow formation instead of droplets was observed at high Q_d/Q_c for the device without a step. Plots of (*b*) volume and (*c*) generation frequency of the droplets as a function of Q_d at a fixed Q_c (40 μL min^{-1} for the devices with a step or 20 μL min^{-1} without a step). The device without a step exhibits a narrow working range (limited to low Q_d) in which droplets can be generated. Beyond this range, no droplet can be formed.

compared in terms of average volume and frequency of droplets generated.

As shown in figure 5(*a*), O/W droplets could be formed at the junction in non-silanized devices with and without a step structure at a low Q_d/Q_c of 0.025 where Q_d refers to the flow rate of the dispersed phase and Q_c is the flow rate of the continuous phase. At a high Q_d/Q_c of 0.400, O/W droplets could still be formed in the devices with either a flat or triangular step structure. In contrast, the device without a step structure could not form droplets under this condition. A thread flow of the dispersed phase was formed instead. This observation was also reflected in figures 5(*b*) and (*c*). The graphs showed that O/W droplets could be generated over a broad range of Q_d (1–16 μL min^{-1}) at a fixed Q_c of 40 μL min^{-1} for the devices with either a flat or a triangular step structure. However, the device without a step structure could only make droplets under a fairly limited range of Q_d (0.5–1 μL min^{-1}). For the device without a step structure, Q_c was fixed at 20 μL min^{-1} instead of 40 μL min^{-1} so as to achieve an equivalent flow velocity for a given shallower channel depth (50 μm).

The average volume and the generation frequency of the O/W droplets increased with Q_d as shown in figures 5(*b*) and (*c*), respectively. Interestingly, the droplets obtained from a flat step profile had a larger average volume compared to those from a triangular step under the same flow rate. The device without a step produced the smallest droplets among all the three. The droplet generation frequency was the lowest for a flat step, followed by a triangular step, and then the structure without a step. Here, the step geometry played a significant role in determining the average volume and the generation frequency of the droplets.

Similar experimental observations were made during the generation of W/O droplets with the silanized devices (figure 6). Without silanization, the devices, despite having a step structure, did not succeed in generating W/O droplets as much as the devices silanized ceased to produce O/W droplets. Using a step structure, the W/O droplets could be generated for a broader range of Q_d. The presence of the step structure and its shape were also shown to have a direct impact on the volume of the W/O droplets as well as their generation frequency.

The capability of a step structure in generating droplets for a broader range of dispersed flow rate might be due to a step-induced instability in the flow-focusing mechanism. Previously, several groups studied the formation of droplets by utilizing the flat step structure downstream from the flow-focusing junction or the T-junction [10, 14, 15]. At high Q_d/Q_c, they created a laminar thread flow of the dispersed phase and enabled the production of droplets at and beyond the step structure. They attributed the formation of droplets to the sudden change in the aspect ratio and to the Rayleigh–Plateau instability [10, 14]. Here, each of our devices had the step structure positioned directly at the flow-focusing junction. Therefore, the droplets could possibly be formed by the combined effect of the flow-focusing mechanism and a step-induced instability.

Droplets of higher volume were generated in the device with a flat step structure compared to the one with a triangular step structure partly because of the difference in the available space in the flow-focusing junction. As the dispersed phase grew into a blob shape at the flow-focusing junction, it would constrict the flow of the continuous phase through the two side channels and hence resulted in a pressure build-up upstream. Upon reaching a critical value, the pressure upstream pinched off the dispersed phase, breaking off the blob to form a droplet. The blob from the flat step was observed to have larger room to grow as it hung over a single flat edge while the blob from the triangular step had less room to grow as it hung over the extended sharp end of the step structure. Given the larger space to grow before it can constrict the flow through the side channels, the blob from the flat step emanates larger droplet than those from the triangular step.

Similarly, the geometry of the step structure could also be used to manipulate the generation frequency of the droplets. As the devices with a flat step and a triangular step structure were compared under an equivalent flow rate, the device that generated smaller droplets would respectively exhibit a higher generation frequency to meet the requirement of the constant volumetric flow rate imposed on the dispersed phase. As a result, the device with a triangular step structure would return a higher generation frequency because of the size of droplets smaller than those by the device with a flat step.

The devices capped with PDMS were also studied for droplet generation. These devices were used under two different conditions: (1) immediately after oxygen plasma treatment for a hydrophilic PDMS surface and (2) after being left overnight in ambient environment to allow the PDMS capping to regain its hydrophobic surface. Under both conditions, the SiO_2 walls remained hydrophilic.

When the surface of the PDMS capping was hydrophilic, the production of O/W droplets was observed. This was expected because the PDMS surface along with the three

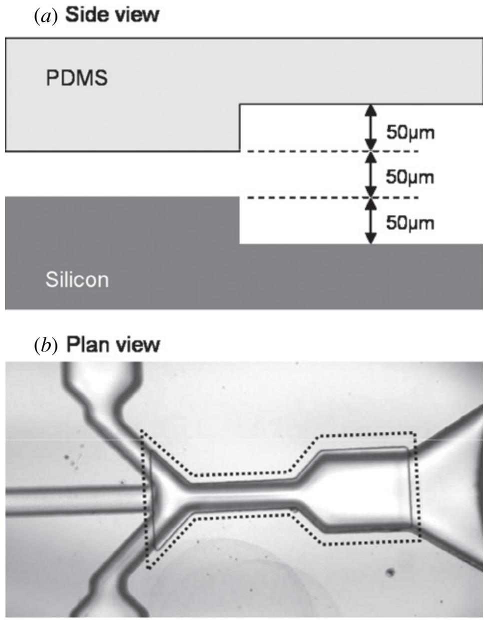

Figure 7. Dual-step flow-focusing junction: (*a*) cross-sectional schematic along the axis of symmetry and (*b*) photomicrograph planar view (dots encloses the upper step profile created in the PDMS cap).

SiO_2 sides of the channel was hydrophilic. The hydrophilic nature causes the aqueous phase, instead of the oil, to wet the surface resulting in O/W droplets. Interestingly, when the surface of the PDMS capping recovers its hydrophobic nature, W/O droplets were able to form despite the hydrophilic state of the SiO_2 walls. For this hybrid configuration of surface wettabilities, the top surface appeared to be dictating the type of droplets being formed.

The step structure seems to be responsible for this observation, at first. As the channel depth expands suddenly right after the step, the dispersed phase (aqueous dye) can separate itself from the bottom surface which is hydrophilic while the oil phase supplied from the two side channels prevents the aqueous phase from touching the hydrophilic walls. Thus, W/O droplets might form due to this geometric effect.

In order to test this hypothesis, a 50 μm deep step was also created in the PDMS cap by soft lithography, as described in figure 7, so as to separate the disperse phase from the capping surface as well. The device was however still observed to produce only W/O droplets and not able to generate O/W droplets without any surface modification. Given this observation, the wettability of the top surface, instead of the step structure, appeared to be the dominant factor that resulted in the formation of W/O droplets. For such channel with hybrid surface wettability, the oil might be wetting the top PDMS surface more than the aqueous dye wetting the SiO_2 surface. As a result, the formation of W/O droplets was favored over O/W droplets as the wettability of one surface dominates over another to determine the type of droplets being formed.

4. Conclusion

In this work, a microfluidic-based droplet generation device with a step profile positioned directly at the flow-focusing junction was demonstrated. A two-step silicon etching method was developed to create the step structure at the flow-focusing junction. In this method, undesirable silicon spikes were encountered at the edge of the step structure. In order to remove these spikes, combination of oxygen plasma ashing and silicon isotropic etching was applied.

Using the devices capped with glass, this work also investigated the effects of having the step structure at the flow-focusing junction on the characteristics of droplet generation behavior. The device with a step structure (either flat or triangular) was able to generate W/O and O/W droplets over a broader dynamic range compared to a device without a step structure. Regarding the step profile, the device with a flat step structure was found to produce larger droplets and at a lower generation frequency compared to the device with a triangular step structure. This showed that the geometry of the step introduced at the flow-focusing junction could be used to control the droplet generation process and to broaden the dynamic range.

PDMS as a capping material on the hydrophilic microchannels in silicon was also investigated. The surface characteristic (hydrophobic or hydrophilic) of the PDMS capping appeared to determine the type of droplets (W/O or O/W) to be formed. This was due to the preferential wetting of oil or water on one surface over another.

References

[1] Mezzenga R, Schurtenberger P, Burbridge A and Michel M 2005 Understanding foods as soft materials *Nat. Mater.* **4** 729–40

[2] Antonietti M and Tauer K 2003 90 years of polymer latexes and heterophase polymerization: more vital than ever *Macromol Chem. Phys.* **204** 207–19

[3] Tadros T F 1993 Industrial applications of dispersions *Adv. Colloid Interface Sci.* **46** 1–47

[4] Teh S-Y, Lin R, Hung L-H and Lee A P 2008 Droplet microfluidics *Lab Chip* **8** 198–220

[5] Thorsen T, Roberts R W, Arnold F H and Quake S R 2001 Dynamic pattern formation in a vesicle-generating microfluidic device *Phys. Rev. Lett.* **86** 4163–6

[6] Tice J D, Song H, Lyon A D and Ismagilov R F 2003 Formation of droplets and mixing in multiphase microfluidics at low values of the Reynolds and the capillary numbers *Langmuir* **19** 9127–33

[7] Nisisako T, Toni T and Higuchi T 2002 *Proc. Soc. of Instrument and Control Engineers Annu. Conf. (Osaka)* pp 957

[8] Anna S L, Bontoux N and Stone H A 2003 Formation of dispersions using 'flow focusing' in microchannels *Appl. Phys. Lett.* **82** 364–6

[9] Seo M, Paquet C, Nie Z, Xu S and Kumacheva E 2007 Microfluidic consecutive flow-focusing droplet generators *Soft Matter* **3** 986–92

[10] Saeki D, Sugiura S, Kanamori T, Sato S, Mukataka S and Ichikawa S 2008 Highly productive droplet formation by anisotropic elongation of a thread flow in a microchannel *Langmuir* **24** 13809–13

[11] Tan Y-C, Cristini V and Lee A P 2006 Monodispersed microfluidic droplet generation by shear focusing microfluidic device *Sensors Actuators* B **114** 350–6

[12] Yobas L, Martens S, Ong W-L and Ranganathan N 2006 High-performance flow-focusing geometry for spontaneous generation of monodispersed droplets *Lab Chip* **6** 1073–9

[13] Ong W-L, Hua J, Zhang B, Teo T-Y, Zhuo J, Nguyen N-T, Ranganathan N and Yobas L 2007 Experimental and computational analysis of droplet formation in a high-performance flow-focusing geometry *Sensors Actuators* A **138** 203–12

[14] Priest C, Herminghaus S and Seemann R 2006 Generation of monodisperse gel emulsions in a microfluidic device *Appl. Phys. Lett.* **88** 024106

[15] Chan E M, Alivisatos A P and Mathies R A 2005 High-temperature microfluidic synthesis of CdSe nanocrystals in nanoliter droplets *J. Am. Chem. Soc.* **127** 13854–61

[16] Utada A S, Lorenceay E, Link D R, Kaplan P D, Stone H A and Weitz D A 2005 Monodisperse double emulsions generated from a microcapillary device *Science* **308** 537–41

[17] Nie Z H, Xu S Q, Seo M, Lewis P C and Kumacheva E 2005 Polymer particles with various shapes and morphologies produced in continuous microfluidic reactors *J. Am. Chem. Soc.* **127** 8058–63

[18] Bocanegra R, Sampedro J L, Ganan-Calvo A and Marquez M 2005 Monodisperse structured multi-vesicle microencapsulation using flow-focusing and controlled disturbance *J. Microencapsulation* **22** 745–59

[19] Abate A R, Krummel A T, Lee D, Marquez M, Holtze C and Weitz D A 2008 Photoreactive coating for high-contrast spatial patterning of microfluidic device wettability *Lab Chip* **8** 2157–60

[20] Xu J H, Li S W, Tan J, Wang T J and Luo G S 2006 Controllable preparation of monodisperse O/W and W/O emulsions in the same microfluidic device *Langumir* **22** 7943–6

[21] Morra M, Occhiello E, Marola R, Garbassi F, Humphrey P and Johnson D 1990 On the aging of oxygen plasma-treated polydimethylsiloxane surfaces *J. Colloid Interface Sci.* **137** 11–24

[22] Nie Z H, Seo M, Xu S Q, Lewis P C, Mok M, Kumacheva E, Whitesides G M, Garstecki P and Stone H A 2008 Emulsification in a microfluidic flow-focusing device: effect of viscosities of the liquids *Microfluid. Nanofluid.* **5** 585–94